Available online at www.sciencedirect.com

SCIENCE DIRECT

Experimental Cell Research 304 (2005) 365–379

Experimental Cell Research

www.elsevier.com/locate/yexcr

Localization of UDP-GlcNAc 2-epimerase/ManAc kinase (GNE) in the Golgi complex and the nucleus of mammalian cells

Sabine Krause[a], Stephan Hinderlich[b], Shira Amsili[c], Rüdiger Horstkorte[b], Heinz Wiendl[d], Zohar Argov[e], Stella Mitrani-Rosenbaum[c], Hanns Lochmüller[a,*]

[a]*Friedrich-Baur-Institute, Department of Neurology and Gene Center, Ludwig-Maximilians-University, Genzentrum München, Feodor-Lynen-Str. 25, 81377 München, Germany*

[b]*Charité-Universitätsmedizin Berlin, Campus Benjamin Franklin, Institut für Biochemie und Molekularbiologie, Berlin-Dahlem, Germany*

[c]*The Goldyne-Savad Institute of Gene Therapy, Hadassah-Hebrew University Medical Center, Jerusalem, Israel*

[d]*Department of Neurology, University of Tübingen, Tübingen, Germany*

[e]*Department of Neurology, Hadassah-Hebrew University Medical Center, Jerusalem, Israel*

Received 21 April 2004, revised version received 31 October 2004
Available online 19 December 2004

Abstract

The bifunctional enzyme UDP-*N*-acetylglucosamine-2-epimerase/*N*-acetylmannosamine kinase (GNE) is essential for early embryonic development and catalyzes the rate limiting step in sialic acid biosynthesis. Although epimerase and kinase activities have been attributed to GNE, little is known about the regulation, differential expression, and subcellular localization of GNE in vivo. Mutations in GNE cause a rare inherited muscle disorder in humans called hereditary inclusion body myopathy (HIBM). However, the role of GNE in HIBM pathogenesis has not been defined yet. Here, we show that the GNE protein is expressed in various mammalian cells and tissues with highest levels found in cancer cells and liver. In human skeletal muscle, GNE protein is developmentally regulated: high levels are found in immature myoblasts but low levels in mature skeletal muscle. The GNE protein colocalizes with resident proteins of the Golgi compartment in a variety of human cells including muscle. Drug-induced disruption of the Golgi and subsequent recovery reveals co-distribution of GNE along with Golgi-targeted proteins. This subcellular localization of GNE is in good agreement with its established role as the key enzyme of sialic acid biosynthesis, since the sialylation of glycoconjugates takes place in the Golgi complex. Surprisingly, GNE is also detected in the nucleus. Upon nocodazole treatment, GNE redistributes to the cytoplasm suggesting that GNE may act as a nucleocytoplasmic shuttling protein. A regulatory role for GNE shifting between the nuclear and the Golgi compartment is proposed. Further insight into GNE regulation may promote the understanding of HIBM pathogenesis.

Keywords: UDP-*N*-acetylglucosamine-2-epimerase/*N*-acetylmannosamine; GNE; Subcellular localization; Brefeldin A; Nocodazole; Golgi; Hereditary inclusion body myopathy; HIBM

Introduction

Sialic acids are located on the distal side of glycan chains in many vertebrate cell surface glycoconjugates and play important roles in regulating glycoprotein stability [1]. They are crucial in controlling cellular interactions, including cell adhesion [2], modulation of surface recognition determinants [3,4], and B-cell signaling [5]. In addition, sialic acids have been implicated in pathogenic processes such as inflammation [6,7], adhesion of viruses or bacteria to target cells [8–10], tumorigenesis, and metastasis [11,12]. Mutations in GNE, the key enzyme of sialic acid biosynthesis, are implicated in human genetic disorders, such as sialuria (OMIM 269921), hereditary inclusion body myo-

Abbreviations: BFA, Brefeldin A; GNE, UDP-*N*-acetylglucosamine-2-epimerase/*N*-acetylmannosamine kinase; HIBM, hereditary inclusion body myopathy; HPA, *Helix pomatia* agglutinin; Neu5Ac, *N*-acetylneuraminic acid; PDI, protein disulfide isomerase; WGA, wheat germ agglutinin.

* Corresponding author. Fax: +49 89 2180 76999.
E-mail address: hanns@lmb.uni-muenchen.de (H. Lochmüller).

0014-4827/$ - see front matter © 2004 Elsevier Inc. All rights reserved.
doi:10.1016/j.yexcr.2004.11.010

pathy (HIBM), and Nonaka myopathy (OMIM 603824). Inactivation of sialic acid biosynthesis by gene targeting causes early embryonic lethality in mice [13].

N-Acetylneuraminic acid (Neu5Ac) is the most abundant naturally occurring sialic acid and serves as a precursor substrate for the entire class of compounds. In the mammalian system, sialic acid biosynthesis resulting in Neu5Ac and its activated form CMP-Neu5Ac is accomplished by five consecutive enzymatic steps (for review, see Ref. [14]). The key enzyme of the sialic acid biosynthetic pathway is the bifunctional UDP-*N*-acetylglucosamine-2-epimerase/*N*-acetylmannosamine kinase (GNE) catalyzing the two initial steps of sialic acid biosynthesis [15], thus determining the extent of cell surface sialylation in human cells [16]. The final step, the activation of Neu5Ac to the sugar nucleotide CMP-Neu5Ac is catalyzed by CMP-Neu5Ac synthetase thereby providing the substrate for Golgi-resident sialyltransferases. Although the sialic acid biosynthetic pathway has been known for more than 30 years [17], the subcellular localization of the essential enzymes in mammals remained elusive. In the mammalian pathway, only GNE and CMP-Neu5Ac synthetase have been characterized at the molecular level. CMP-Neu5Ac synthetase has been found almost exclusively in the cell nucleus [18,19] suggesting that nucleocytoplasmic shuttling of substrate intermediates might be involved in sialic acid biosynthesis.

Nucleocytoplasmic exchange occurs via dedicated multiprotein structures spanning the nuclear envelope, termed 'Nuclear Pore Complexes' (NPCs). Two types of transport are mediated by the NPC. Passive diffusion allows the exchange of ions and small molecules, including proteins smaller than 40–60 kDa, while the translocation of larger proteins or protein complexes is controlled by nuclear localization signals (NLSs) and nuclear export signals (NESs). These motifs are recognized by soluble import and export receptors, which can associate with nucleoporins in the NPC, thus leading to transport of cargo across the nuclear membrane (for review, see Ref. [20]). The most common NES is a short stretch of characteristically spaced hydrophobic amino acids as first described for the human immunodeficiency virus type 1 Rev and PKI proteins [21,22].

The precise subcellular localization of the key enzyme of sialic acid biosynthesis, GNE, has not been investigated yet. In the present study, we show cytoplasmic targeting of GNE to the Golgi complex. Unexpectedly, prominent nuclear localization was detected as well suggesting additional functional roles for GNE.

Materials and methods

Cell lines and cell culture

All cell lines were obtained from the American Type Culture Collection (ATCC, Manassas, VA, USA) except for human myoblasts (Muscle Tissue Culture Collection, Friedrich-Baur-Institute, Munich, Germany). HeLa cells (human cervical epithelioid carcinoma), HEK 293 cells (human embryonal kidney), and TE671 cells (human rhabdomyosarcoma) were grown in Dulbecco's modified Eagle medium (DMEM) supplemented with 2 mM L-glutamine, 50 IU/ml penicillin, 50 mg/ml streptomycin (PAA, Linz, Austria), and 10% FCS (GibcoBRL, Eggenstein, Germany). Human myoblasts were grown in skeletal muscle growth medium, (SGM PromoCell, Heidelberg, Germany) supplemented with 15% FCS. Jurkat cells (human leukemia T cells) and K562 cells (human erythroleukemia) were grown as suspension cultures in RPMI 1640 (GibcoBRL) supplemented with 10% FCS. Murine embryonic stem cells carrying a homozygous or heterozygous GNE gene knock-out were grown in monolayer as described [13].

For immunofluorescence staining, myoblasts were grown in SGM on glass coverslips coated with bovine collagen (Sigma). For maturation into multinucleated myotubes, they were grown in SGM on coverslips coated with laminin (Sigma) to near confluency and were induced to fuse and differentiate by replacing SGM with DMEM supplemented with 2% horse serum (fusion medium) for 48 h. For drug treatment experiments, cells were incubated with 5 μg/ml brefeldin A (BFA) or 30 μM nocodazole for the times indicated. For recovery, the cells were washed once in DMEM supplemented with 10% FCS and maintained in the same medium.

Antibodies and reagents

A polyclonal antiserum was raised in rabbit against a GNE peptide (Sigma-Genosys, Cambridgeshire, UK) comprising amino acids 588–607 coupled to keyhole limpet hemocyanine (KLH) and affinity-purified against the corresponding antigenic peptide. Mouse monoclonal antibodies against golgin-97 (1 μg/ml) was purchased from Molecular Probes (Leiden, The Netherlands), anti-protein disulfide isomerase (anti-PDI, 5 μg/ml) was from Stressgen (Victoria, Canada), and anti-CBP (anti-CREB-binding protein) was purchased from Santa Cruz Biotechnology (Santa Cruz, CA). Monoclonal antibodies against dystrophin rod domain (Dys1, amino acids 1181–1388), C-terminal domain (Dys2, amino acids 3669–3685), and actin binding domain (Dys3, amino acids 321–494) were from Novocastra Laboratories (Newcastle upon Tyne, UK). The secondary antibodies (Dianova, Hamburg, Germany) were used as follows: fluorescein (FITC)-conjugated donkey anti-mouse (1:100), Cy3-conjugated goat anti-rabbit (1/200), and Texas Red-conjugated donkey anti-rabbit (1:200). Nuclei were visualized using bisbenzimide H 33258 (40 μg/ml; Sigma).

Nocodazole and brefeldin A (BFA) were purchased from Sigma. Stock solutions of nocodazole in DMSO (30 mM) and brefeldin A in absolute ethanol (10 mg/ml) were kept

in aliquots at −80°C. Lectins conjugated to Alexa Fluor 488, *Helix pomatia* agglutinin (HPA) and wheat germ agglutinin (WGA), were purchased from Molecular Probes. Recombinant rat GNE was expressed in Sf9 insect cells and purified as described [23].

Immunofluorescence staining

Coverslips were briefly washed in PBS and fixed in 3.7% formaldehyde (freshly prepared from paraformaldehyde) in cytoskeleton (CSK) buffer, a microtubule-stabilizing buffer (10 mM piperazine-*N,N*'-bis(2-ethanesulfonic acid), 100 mM NaCl, 10% sucrose, 10 mM EGTA, 2 mM $MgCl_2$ in water at pH = 6.8) for 15 min at room temperature. Permeabilization was in 0.5% Triton X-100 in CSK buffer for 10 min. After three washes in PBS, blocking of unspecific binding sites with 10% horse serum in phosphate-buffered saline (PBS) for 1 h was followed by incubation with the primary antibodies diluted in PBS containing 5% horse serum for 1 h in a humid chamber. After three washes in PBS, the cells were incubated with the appropriate secondary antibodies conjugated to fluorescein isothiocyanate (FITC), Texas Red or Cy3. Alternatively, for lectin staining, the cells were labeled with Alexa Fluor 488-conjugated HPA or WGA (100 μg/ml). Finally, the coverslips were mounted in DAKO fluorescent mounting medium (DAKO, Carpinteria, CA, USA) and sealed with nail polish.

Monolayer cells were analyzed and photographed using a Zeiss Axiovert 200 M fluorescence microscope and a Zeiss AxioCam HR photocamera. For confocal laser scanning fluorescence microscopy, slides were evaluated with a Krypton-Argon laser (Leica TCS NT System, Leica Microsystems, Mannheim, Germany) attached to a Leica DM IRB/E fluorescence microscope. Specificity controls consisted of replacement of primary antibodies by non-immune serum and of omitting the primary antibodies.

Retroviral transfection

The cDNA encoding the entire human GNE protein fused to an N-terminal $(FLAG)_3$-epitope was cloned into the retroviral expression vector pLXSN (BD Biosciences Clontech, Heidelberg, Germany) related to the Moloney murine leukemia virus under the control of a CMV (cytomegalovirus) promoter. An amphotropic retrovirus was obtained by subsequent passaging in two producer cell lines (GP+E-86 and pA317 Ref. [24]). The titer was 1.6×10^5. $(FLAG)_3$-GNE protein expression in the virus producer cell line was corroborated by immunoblot analysis of cell lysates detected with anti-FLAG (see below) and anti-GNE antibodies. Retroviral infection of HeLa cells was done at an multiplicity of infection (MOI) of 10–20 in DMEM without FCS containing 4 μg/ml polybrene (hexadimethrine bromide, Sigma) for 6 h. For immunofluorescence staining, the recombinant protein was labeled with mouse anti-FLAG M2 monoclonal antibody (20 μg/ml, Sigma) and detected with FITC-conjugated donkey anti-mouse antibody (1:100, Dianova).

Immunoblotting, peptide competition experiment, and cell fractionation

Cells were lysed at 4°C in lysis buffer (20 mM Tris–HCl pH 7.6, 1% NP-40, 150 mM NaCl, 1 mM EDTA) including freshly added protease inhibitors (1 mM phenymethyl sulfonylfluoride, 0.5 μg/ml leupeptin, 0.7 μg/ml pepstatin, 1 mM benzamidine, Sigma). Flash frozen mouse tissues (6 month, C57BL/6) were ground to a fine powder in a mortar using liquid nitrogen that was subsequently solubilized in the same lysis buffer. After removal of cell debris by centrifugation, protein content of the lysates was quantified by the bicinchoninic acid method [25] using the BCA assay reagent kit (Uptima, interchim, Montluçon, France). Lysates equivalent to 30 μg total protein were separated by denaturing 7.5% SDS-PAGE and transferred to nitrocellulose (Schleicher and Schuell, Dassel, Germany) using standard immunoblotting techniques. GNE was labeled with the affinity-purified polyclonal rabbit antibody (10 μg/ml) for 1 h at room temperature. Immunoreactive bands were detected by enhanced chemiluminescence after incubation with horseradish peroxidase-conjugated goat anti-rabbit secondary antibody (1:7000; Dianova). Each immunoblot was repeated at least three times for independent samples.

A peptide competition experiment was performed by Western blot analysis using 20 μg of affinity-purified anti-GNE antibody in the presence of 1.3 and 13 μg synthetic GNE peptide (amino acids 588–607) corresponding to a molar excess of 1:100 and 1:1000, respectively. Cytoplasmic and nuclear fractions of HeLa cells were prepared according to Ref. [26].

Computational analysis

The method of Cokol et al. [27] was performed to search for putative nuclear localization signals.

Results

Differential GNE protein expression in mammalian cells and tissues

A polyclonal GNE antiserum was raised in rabbit against a GNE peptide (aa 588–607). This peptide sequence is conserved in human, rat and mouse. On Western blots, a single protein band of about 79 kDa is detected in crude extracts of mouse liver or fetal human myoblasts (Fig. 1A). A dilution series of recombinant His_6-tagged GNE analyzed on the same Western blot demonstrates that the GNE antiserum readily detects as

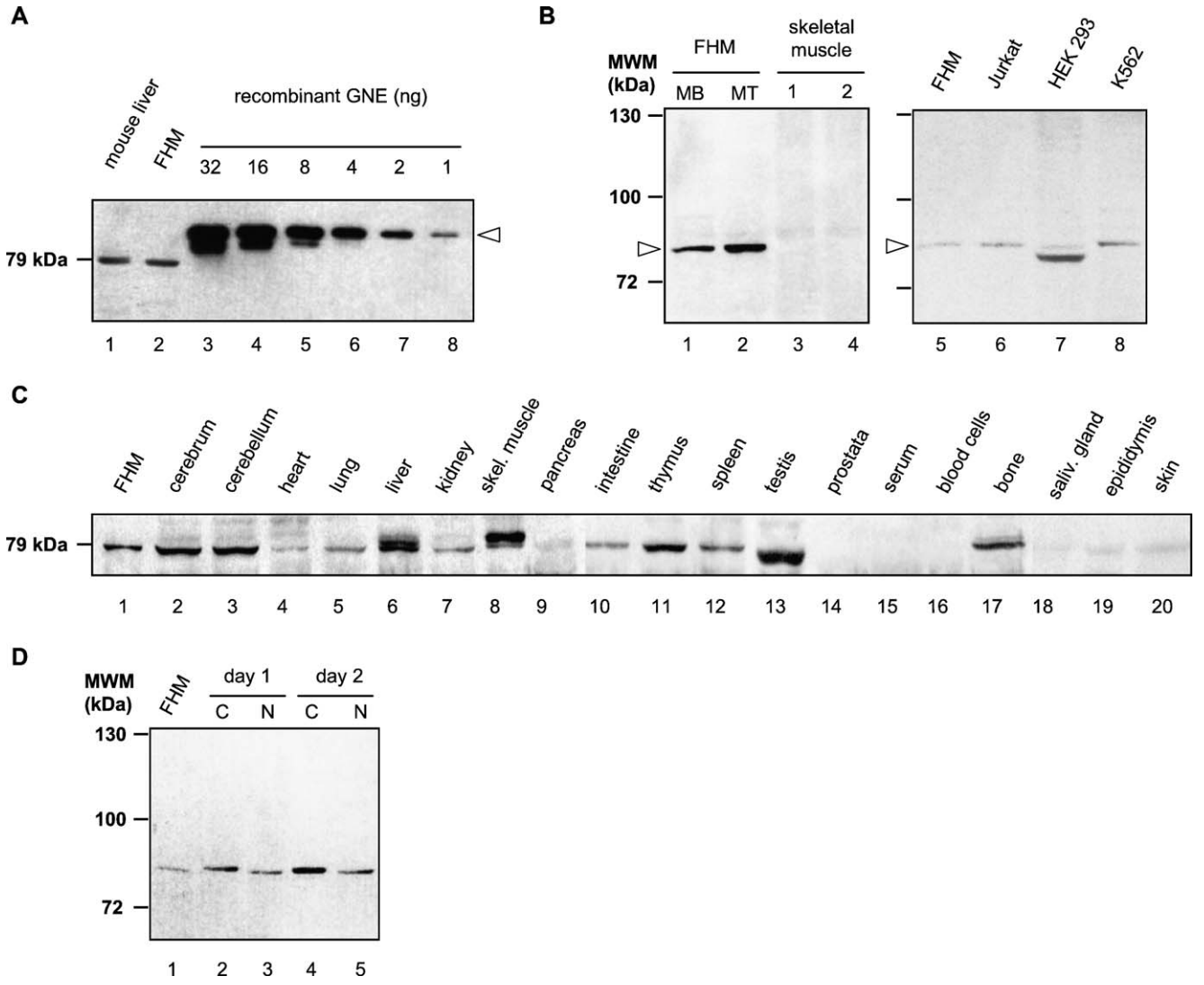

Fig. 1. Western blot detection of GNE. (A) Mouse liver and fetal human myoblast (FHM) total cell extracts (lanes 1 and 2; 7.5 μg total protein each) and a dilution series of purified recombinant rat GNE corresponding to 32, 16, 8, 4, 2, and 1 ng protein (lanes 3–8) was separated on a 7.5% SDS-polyacrylamide gel followed by blotting to nitrocellulose. GNE was detected with an affinity-purified antiserum against aa 588–607 of GNE. As little as 1 ng recombinant GNE is detected by the GNE antiserum. Note that the recombinant rat GNE has a higher apparent molecular weight than the murine or human wild type protein due to a $(histidine)_6$-tag (open arrow head). The double band in lanes 3–6 is possibly due to a posttranslational modification of the recombinant GNE protein in insect cells. In mouse liver and in FHM total cell extracts, the antibody specifically labeled a single 79-kDa protein. (B) GNE is highly expressed in fetal human myoblasts and myotubes in vitro (lanes 1 and 2), and at lower levels in mature skeletal muscle (M. biceps brachii, lanes 3 and 4). Moreover, GNE is highly expressed in a variety of human cancer and embryonal cell lines like Jurkat cells, human embryonal kidney cells (HEK293), and erythroleukemia cells (K562) in lanes 6–8. Please note that total protein loading was 30 μg 1–4, whereas only 15 μg were loaded in lanes 5–8. FHM total cell extracts show a single 79-kDa band corresponding to GNE (open arrowhead). (C) Murine multiple tissue Western blot. The GNE protein is differentially expressed in a variety of murine tissues with cerebrum, cerebellum, liver, skeletal muscle (quadriceps muscle), thymus, and testis exhibiting the highest GNE protein level. FHM total cell extract (15 μg total protein) served as a control (lane 1). Note that GNE appears as a double band in liver and skeletal muscle. Panel C was assembled from three separate immunoblots. (D) Cell fractionation of HeLa cells, harvested on day 1 (50% confluency) and day 2 following seeding. Cytoplasmic (C) and nuclear fractions (N) normalized for total protein were analyzed by immunoblotting. Thirty micrograms total protein was analyzed in panels (A)–(D) unless stated otherwise.

little as 1 ng GNE protein (Fig. 1A). The recombinant GNE migrates slower than the wild type protein (mouse liver and human myoblasts) due to the addition of a His_6-tag. A double band in the recombinant GNE preparation is evident if large protein amounts are loaded (Fig. 1 lanes 3–6), probably as a result of an unidentified posttranslational modification in insect cells. Competition experiments including preincubation of the antibody with both 100- and 1000-fold molar excess of the immunogenic peptide completely abolish the specific 79-kDa signal (data not shown). Murine embryonic stem cells carrying a GNE gene knock-out [13] completely lack the 79-kDa signal that is present both in wild type and in heterozygous knock-out cells (data not shown). Therefore, we conclude that the antiserum specifically detects a protein corresponding to GNE.

Immunoblot analysis of crude cell extracts from fetal human myoblasts and myotubes reveals high expression of GNE (Fig. 1B, lanes 1 and 2). A weaker GNE signal is present in extracts from human skeletal muscle (Fig. 1B, lanes 3 and 4). Human cancer and embryonal cell lines also show strong GNE expression (Fig. 1B, lanes 6–8).

The GNE protein is differentially expressed in a variety of mouse tissues as shown in a multiple murine tissue Western blot (Fig. 1C) with highest levels in cerebrum, cerebellum, liver, skeletal muscle, thymus, and testis. The GNE signals in liver, skeletal muscle, and testis appear as a double band. This may indicate tissue-specific differences in splicing and/or posttranslational modification.

GNE localizes to the Golgi complex and the nucleus in a variety of human cells

Immunohistochemical analysis of human tissue and cell lines was performed to characterize the specific subcellular localization pattern of GNE. Immunofluorescence microscopy using an affinity-purified anti-peptide antiserum reveals that GNE localizes to nuclear and bright polarized juxtanuclear compartments on cryosections of human skeletal muscle as well as in HeLa cells (Figs. 2A and C). The cytoplasmic juxtanuclear signal is suggestive of the Golgi complex. The antibody specifically detects GNE by immunostaining as shown in a peptide competition experiment. Incubation of the GNE antibody with a synthetic GNE peptide (aa 588–607) prior to immunolabeling abolishes any staining signal in the cytoplasm and the nucleus (Figs. 2B and D). Confocal imaging of human skeletal muscle cryosections simultaneously stained with anti-GNE and anti-dystrophin antibodies demonstrates GNE-labeling of the myonuclei inside the sarcolemma.

Colocalization of the GNE protein with the Golgi apparatus

To investigate the cytoplasmic localization of GNE in more detail, colocalization studies were performed using markers specific for various organelles. Lectins are useful tools for staining Golgi structures by their selective affinity for certain glycoprotein and glycolipid moieties that are processed in the Golgi. *Helix pomatia* agglutinin (HPA) and wheat germ agglutinin (WGA) are specific for terminal *N*-acetylgalactosamine [28] and sialic acid residues [29], respectively. Conventional immunofluorescence analysis of HeLa cells following double labeling of GNE and glycoproteins with Alexa Fluor 488-conjugates of WGA or HPA reveals partial overlap of GNE and lectin staining in bright juxtanuclear structures (Figs. 3A–G) suggestive of the Golgi complex. Additionally, GNE is distributed more diffusely throughout the cytoplasm. To confirm the association of GNE with the Golgi compartment, confocal laser scanning microscopy demonstrates partial colocalization of GNE and golgin-97 (Figs. 3H–J), a Golgi-specific protein [30] that has been suggested to be involved in membrane-tethering functions [31]. Protein disulfide isomerase (PDI) was used as a marker for the endoplasmic reticulum (ER). PDI is an abundant protein of the ER containing a carboxy-terminal KDEL retention

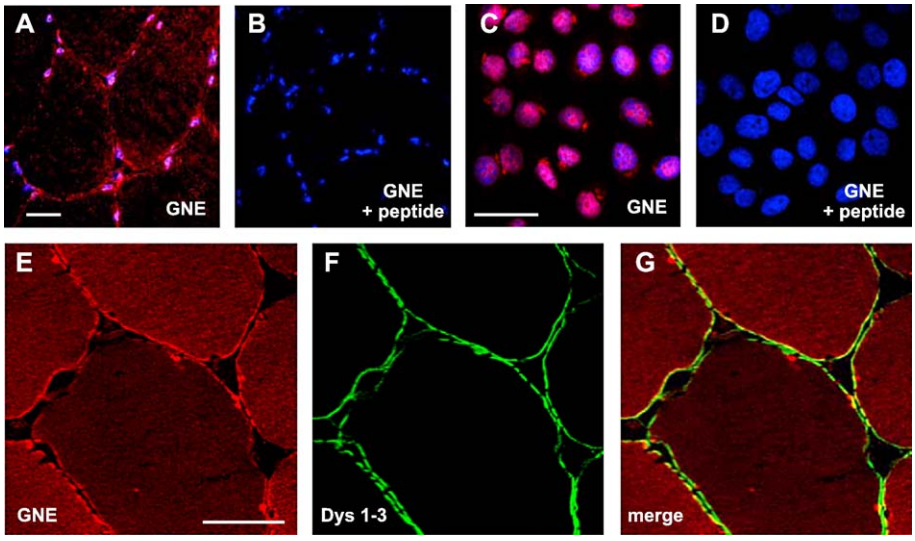

Fig. 2. GNE localizes to nuclear and cytoplasmic juxtanuclear compartments. Human 8 μm-transverse muscle cryosections from the soleus muscle of a 29 year-old male (A, B) and HeLa cells grown on glass coverslips (C, D) were immunostained with an affinity-purified anti-GNE antibody (red, Cy3). Nuclei were simultaneously visualized in blue (bisbenzimide H 33258, 40 μg/ml) and visualized by conventional immunofluorescence microscopy. A competition experiment demonstrates that the specific GNE signal is abolished on transverse muscle sections (B) as well as in HeLa cells (D). Prior to immunostaining, the GNE antibody was preadsorbed to a 1000-fold molar excess of a GNE peptide (aa 588–607). Confocal laser scanning microscopy of human 8 μm-transverse muscle cryosections (E–G) simultaneously labeled with anti-GNE (red, Texas Red) and monoclonal anti-dystrophin antibodies against rod, C-terminal and actin binding domain (Dys1-3, green, FITC) demonstrates that GNE is present in the myonuclei inside the sarcolemma. Scale bar, 10 μm. (For interpretation of the references to colour in this figure legend, the reader is referred to the web version of this article.)

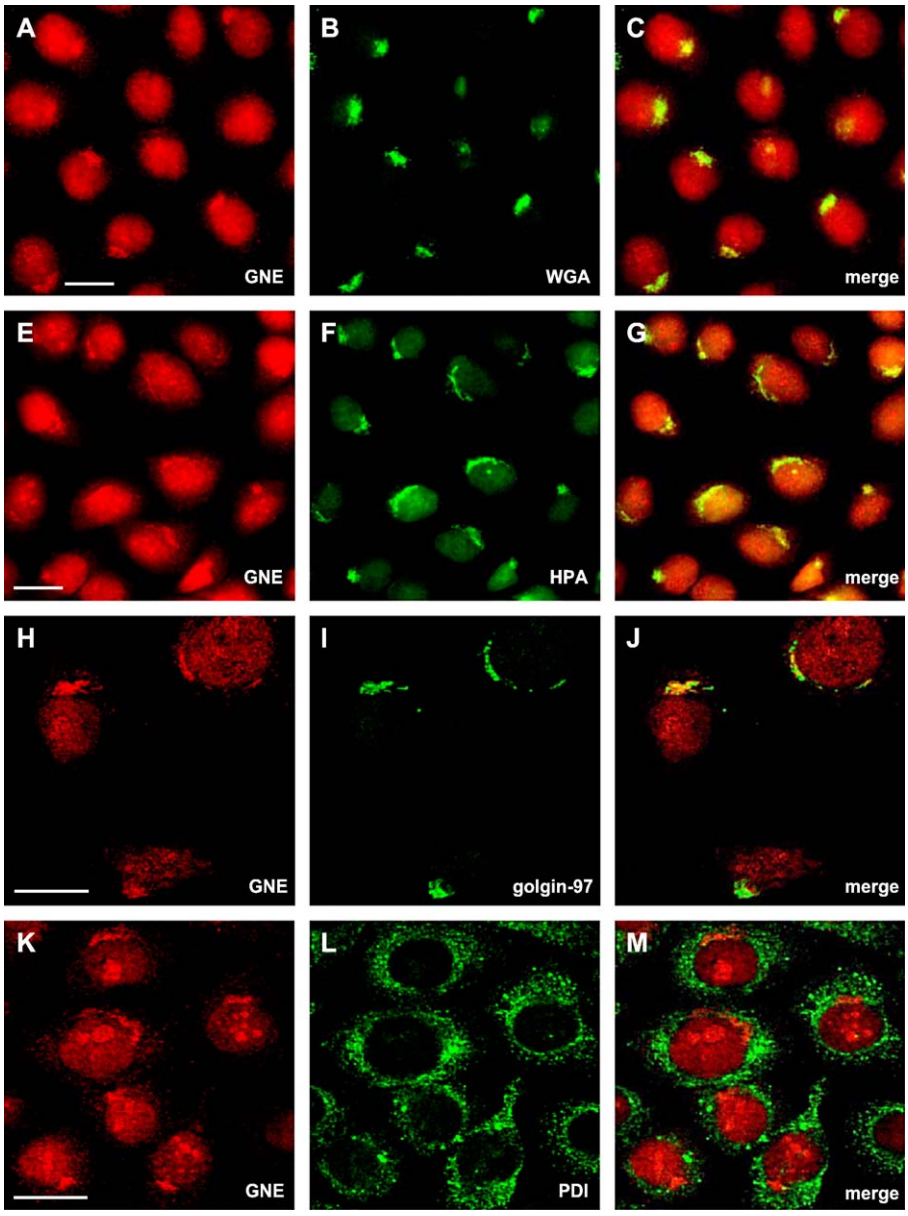

Fig. 3. GNE localizes to the Golgi compartment and the cell nucleus but is not detected in the endoplasmic reticulum. For conventional immunofluorescence microscopy, HeLa cells were double-labeled with an antibody directed against GNE (red, Cy3, A, and E) and Alexa Fluor 488-coupled lectins like WGA (wheat germ agglutin, green, B) decorating *N*-acetylglucosamine and *N*-acetylneuraminic acid residues or HPA (*Helix pomatia* agglutinin, green, F) binding to α-*N*-acetyl-D-galactosamine residues. Overlapping of red and green signals yields a yellowish color (C and G). For confocal fluorescence microscopy analysis, HeLa cells were simultaneously labeled with anti-GNE (red, H) and anti-golgin-97 (green, I). The overlay reveals colocalization of GNE and golgin-97 in the Golgi compartment (yellow, J). Double labeling of cells with anti-GNE (red, K) and anti-PDI (protein disulfide isomerase, green, L), a protein confined to the endoplasmic reticulum, reveals no colocalization in the overlay (M) by confocal laser scanning microscopy. Scale bar, 10 μm. (For interpretation of the references to colour in this figure legend, the reader is referred to the web version of this article.)

signal sequence [32]. Simultaneous immunolabeling of GNE and PDI reveals no marked colocalization (Figs. 3K–M).

Brefeldin A and Nocodazole treatment displaces GNE along with Golgi complex markers

To elucidate the dynamics of the GNE association with Golgi markers, the architecture of the Golgi compartment was disturbed by drug treatment. Brefeldin A (BFA) causes the Golgi stack to disappear by redistributing both protein and lipid components to the ER. Upon BFA treatment of HeLa cells for 1 h, the intense juxtanuclear staining of GNE is abolished (Fig. 4A compare to Fig. 3). GNE is distributed in a punctuated perinuclear and cytoplasmic pattern partially colocalizing with the Golgi marker golgin-97 (Fig. 4C). Following BFA treatment for 1 h, the cells were allowed to recover in the absence of the drug for 1 and 2 h, respectively (Figs. 4D–I). As

visualized by golgin-97 staining, the Golgi compartment recovers its initial distribution (Fig. 4H). Note that the photographs in Fig. 4 were taken at higher magnification and the Golgi compartment appears less compact when compared to Fig. 3I. GNE partially follows the golgin-97 redistribution into the reforming Golgi complex as indicated by co-immunolocalization (Figs. 4F, I). Upon scattering of the Golgi by treatment with the microtubule-depolymerizing drug nocodazole, GNE remained associated with the Golgi marker (Figs. 4J–L). The juxtanuclear array of Golgi complexes is restored subsequent to recovery for 2 h in the absence of the drug (Figs. 4M–O). The nuclear distribution of GNE in HeLa cells during nocodazole treatment and recovery is not homogenous. About half of the cells display widespread intense nuclear staining, whereas the GNE signal is weaker or almost absent in the other half.

Immunolocalization of $(FLAG)_3$-tagged GNE in the Golgi compartment and the nucleus following transfection into HeLa cells

To verify the localization of endogenous GNE observed by immunofluorescence, we analyzed the distribution of a recombinantly expressed N-terminally $(FLAG)_3$-tagged version of GNE. At about 50% confluency, HeLa cells were transfected with an amphotropic retrovirus containing GNE cDNA (coding exons 2–12) under the control of a CMV promoter. The cells were stained simultaneously with an anti-FLAG antibody and the GNE antibody. Confocal laser scanning microscopy revealed colocalization in the Golgi and the nucleus (Fig. 5). Additionally, $(FLAG)_3$-tagged GNE translation products were visualized in several small clusters in the cytoplasm. Unlike endogenous GNE, the FLAG-tagged construct marks the Golgi complex more strongly than the nucleus.

The GNE antibody labels subnuclear domains that undergo changes in response to medium exchange and drug treatment

Unexpectedly, a large fraction of GNE is targeted to the nucleoplasm and a few intensely stained subnuclear domains of HeLa cells as observed by confocal microscopy (Figs. 3A, E, H, K). Upon BFA treatment disrupting the Golgi complex, the nuclear distribution of GNE remains largely unchanged for 1 h (Fig. 4A), when compared to untreated HeLa cells (Fig. 3). During recovery from BFA, intensely staining nuclear domains become prominent after 2 h (Figs. 4D, G). Upon nocodazole treatment and recovery, the nuclear GNE signal is heterogenous in the cell population. Nuclear GNE is nearly missing or weaker in about half of the cells and more prominent in the other half lacking any larger nuclear clusters (Figs. 4J, M).

In general, the GNE-related nuclear staining pattern in HeLa cells was variable (Figs. 3A, E, H, K) and changed rapidly upon recovery from BFA treatment and during exposure to nocodazole (Figs. 4D, G, J, M). These findings prompted us to analyze HeLa cells in culture over time. Cells were seeded at low density and maintained for 6 days with one medium exchange on day 4. For confocal microscopy analysis, the cells were labeled for GNE and golgin-97. The nuclear GNE distribution changes over time including increased cluster formation and a decrease in diffuse nucleoplasmic staining until day 4. The day following medium exchange (day 5), GNE appears diffusely throughout the nucleoplasm concentrating in numerous smaller granules. On day 6, GNE seems again redistributed into 1–3 large, intensely labeled nuclear domains (data not shown).

The relative nucleocytoplasmic distribution of GNE was determined by cell fractionation of HeLa cells 1 and 2 days after seeding. Purity of cytoplasmic and nuclear fractions was confirmed by Western Blot analysis and subsequent immunodetection of golgin-97 as cytoplasmic marker and C responsive element-binding protein (CBP) as nuclear marker protein (data not shown). Cytoplasmic and nuclear fractions were normalized for total protein and separated on a Western blot followed by immunodetection with the GNE antibody (Fig. 1D). Densitometry analysis of the specific immunoblot signals reveals nuclear versus cytoplasmic GNE ratios ranging from 1:1.7 on day 1 and 1:2.3 on day 2.

The subcellular GNE localization in myogenic cells is similar to HeLa cells

To investigate the subcellular targeting of GNE in cells of myogenic origin, TE671 cells, a rhabdomyosarcoma line and fetal human myoblasts (FHM) were double labeled for GNE and a Golgi marker and analyzed by confocal laser scanning microscopy (Figs. 6A–F). Colocalization occurs in an intensely stained juxtanuclear compartment typical of the Golgi complex. Moreover, most of the nuclei are labeled by the anti-GNE antibody (Figs. 6A, D) and display a similar staining pattern like HeLa cells. After maturation of FHM into differentiated, multinuclear myotubes, the Golgi apparatus appears as a vesicular juxtanuclear structure (Figs. 6G–I) that is less compact when compared to myoblasts (Figs. 6D–F). GNE is also present in a widespread nuclear staining pattern in most of the myotubes (Figs. 6G, I).

Brefeldin A redistributes GNE in primary human myoblasts and myotubes along with Golgi markers, whereas Nocodazole displaces GNE and Golgi proteins in myoblasts but not in myotubes

To investigate the dynamic association of GNE with the Golgi compartment and to elucidate GNE targeting changes during myogenesis, primary human myoblasts and myotubes were exposed to BFA and nocodazole. Double

labeling of GNE and the Golgi marker protein golgin-97 reveals colocalization in myoblasts throughout the cytoplasm subsequent to BFA-induced collapse of Golgi stacks appearing more vesiculated (Figs. 7A–C, compare to Fig. 6). The nuclear localization of GNE persists in a widespread nucleoplasmic pattern with some clustering in many small and a few larger nuclear domains. Also, nocodazole treatment has a dramatic effect on disturbing the Golgi

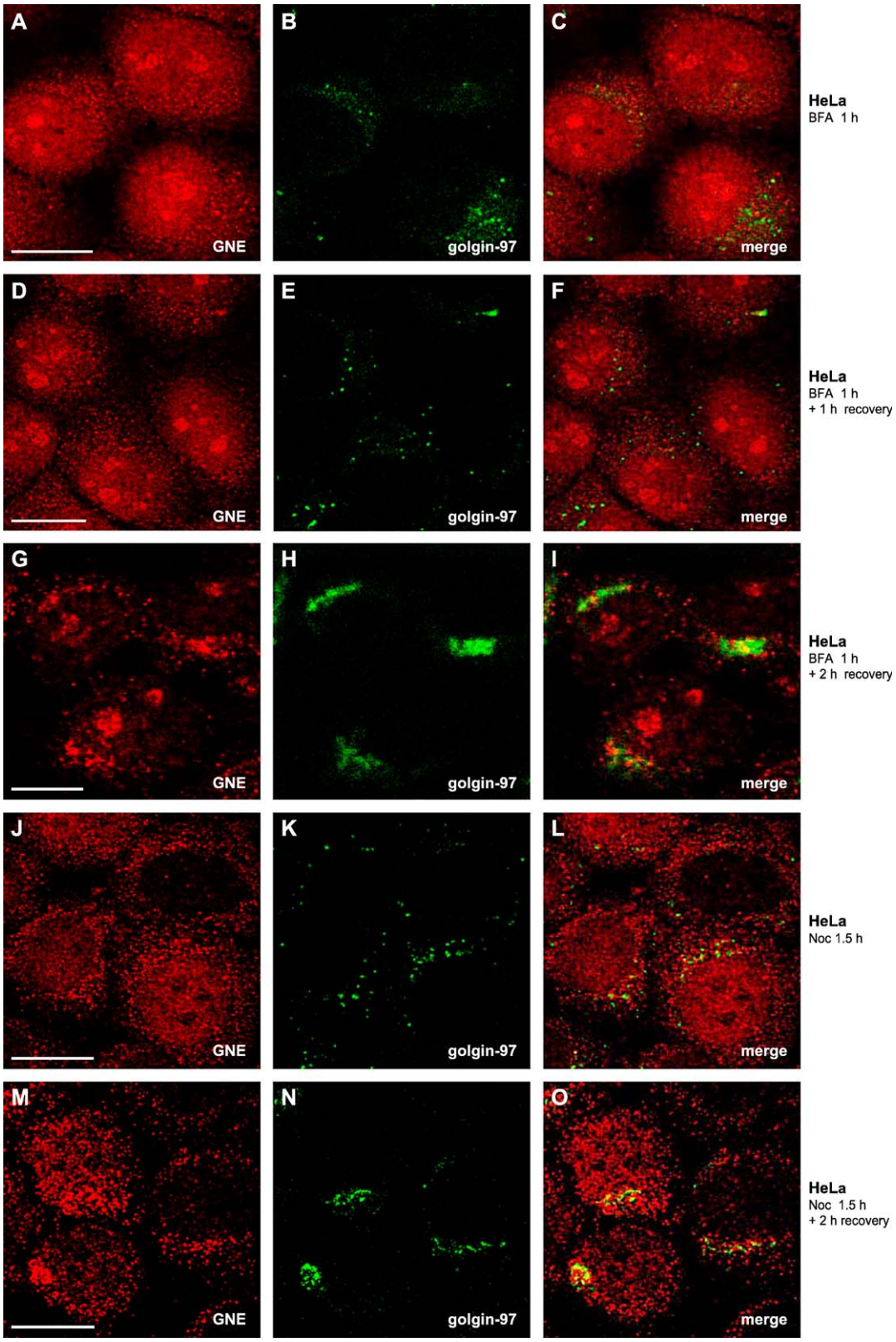

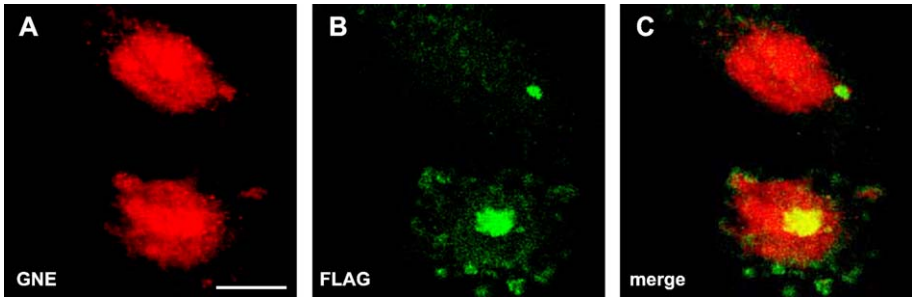

Fig. 5. FLAG-tagged GNE recombinantly expressed in HeLa cells is targeted to the Golgi complex and the nucleus. At about 50% confluency, HeLa cells were transfected with a retrovirus expressing GNE cDNA (coding exons 2–12, GenBank acc. no. AL158830) fused to an N-terminal $(FLAG)_3$-tag under the control of a CMV promoter. The cells were labeled simultaneously with the GNE antibody (red, Texas Red, A) and a monoclonal anti-FLAG antibody (green, FITC, B). Confocal laser scanning microscopy revealed colocalization in the Golgi complex and the nucleus (C). Additionally, the $(FLAG)_3$-tagged GNE was visualized in several small clusters in the cytoplasm that are largely devoid of any prominent GNE-specific staining. The clusters might represent aberrant FLAG-tagged GNE translation products resulting from constitutive overexpression under the CMV promoter or degraded N-terminally tagged GNE-peptides lacking the epitope of the GNE antibody in the kinase domain of GNE. Scale bar, 10 μm. (For interpretation of the references to colour in this figure legend, the reader is referred to the web version of this article.)

morphology in myoblasts with extensive scattering of GNE along with Golgi-related vesicles as visualized by colocalization with golgin-97 (Figs. 7D–F). During recovery from nocodazole exposure, reformation of the Golgi complexes is in progress after 30 min as followed by the marker protein golgin-97. As expected, GNE colocalizes to the reforming Golgi-related compartment (Figs. 7G–I). BFA treatment of differentiated, multinuclear myotubes yields diffuse and vesiculated distribution of GNE along with golgin-97. By contrast, upon exposure to nocodazole, the Golgi morphology in myotubes remains largely unchanged (Figs. 7M–O) when compared to the untreated cells (Figs. 6G–I). GNE remains localized to the Golgi compartment surrounding the myonuclei or concentrating on opposite poles. Note that the Golgi architecture in myotubes is highly variable.

Discussion

The present report provides insight into the tissue distribution and the subcellular compartmentalization of mammalian GNE. So far, these studies were hampered by the lack of an appropriate antiserum to GNE. We now demonstrate tissue-specific regulation of GNE protein expression by Western blotting. Cerebrum, cerebellum, liver, skeletal muscle (quadriceps muscle), thymus, and testis contain the highest amounts of GNE protein in mouse at the expected molecular weight of about 79 kDa. Moreover, undifferentiated cells express high levels of GNE protein in vitro consistent with published results of mRNA expression [33,34]. In agreement with this finding, in rodents, the highest levels of mRNA expression and catalytic activity were found in liver, salivary glands, and intestinal mucosa while in other organs less mRNA expression is detected paralleled by lower total enzyme activities [35].

In accordance with its pivotal role in the sialic acid biosynthesis pathway, it is conceivable that GNE is subject to tight regulation with respect to transcription, translation and multimeric assembly. Protein detection in several tissues with lower or absent biochemical activities may be explained through various mechanisms or factors: (i) allosteric feedback inhibition by CMP-NeuAc, the activated end product of sialic acid biosynthesis, (ii) inactive state, or (iii) higher sensitivity of protein detection by the GNE antiserum. Since GNE mutations cause a primary muscle disorder in human (HIBM), GNE protein expression in mammalian skeletal muscle is conceivable. Upon immunoblotting, the GNE signal of mouse skeletal muscle is much stronger as compared to human muscle. Possibly,

Fig. 4. GNE association with the Golgi compartment is disturbed by brefeldin A (BFA) and Nocodazole. HeLa cells were treated with BFA (1 μg/ml) for 1 h (A–I). Co-immunostaining of GNE (red, Texas Red, A) and golgin-97 (green, FITC, B) followed by confocal microscopy reveals complete disruption of the Golgi apparatus. The superimposition of red and green images shows some BFA-induced redistribution of GNE together with Golgi-associated proteins near the nuclear envelope (yellow, C). In addition, the GNE antibody displays a widespread staining of the nucleus (A and C). The cells depicted in panels D–I were allowed to recover after BFA treatment for the times indicated. One hour following removal of BFA, golgin-97 reclusters in more compact vesicles (E). GNE partially localizes to these vesicles (D) as illustrated by the overlay in yellow (F). Two hours after removal of BFA, the Golgi-apparatus is recovered as monitored by golgin-97 (H). GNE only partially colocalizes with Golgi-specific markers in the overlay (I). A major fraction of GNE is found in the nucleus. Redistribution of GNE to nuclear clusters becomes more prominent 2 h after BFA treatment (compare D and G). Effect of nocodazole on the localization of GNE in HeLa cells (J–O). Double immunolabeling of GNE (J) and golgin-97 (K) after nocodazole treatment (30 μM) for 1.5 h shows the formation of golgin-97-positive cytoplasmic vesicles most of them colocalizing with GNE (L). Additionally, GNE appears prominent in the nucleus in about half of the cells whereas the nuclear GNE signal is weaker or absent in the other half. At 2 h following Nocodazole treatment, the Golgi apparatus is recovered as evidenced by the golgin-97 antibody (N). GNE also partially redistributes to the Golgi compartment as demonstrated in the overlay (O) whereas nuclear GNE staining remains heterogenous (M and O). Scale bar, 10 μm. (For interpretation of the references to colour in this figure legend, the reader is referred to the web version of this article.)

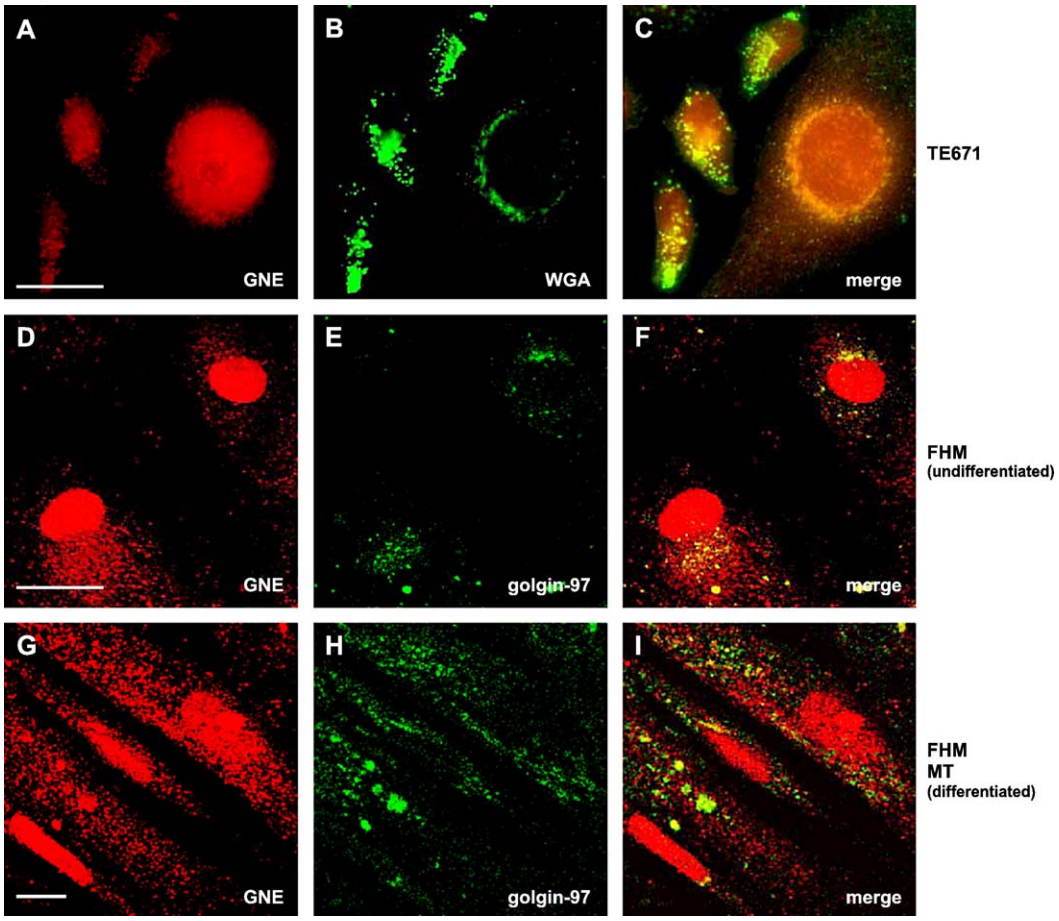

Fig. 6. GNE is partially localized to the Golgi compartment as well as the nucleus of human muscle cells. For immunofluorescence analysis, TE671 (human rhabdomyosarcoma) cells, fetal human myoblasts (FHM), and FHM differentiated into myotubes (MT) were labeled with anti-GNE (A, D, and G) and simultaneously stained with Alexa Fluor 488-conjugated wheat germ agglutinin (B) or golgin-97 (E and H). The overlay of red and green images visualizes colocalization of GNE and Golgi-resident molecules in yellow (A–C, conventional immunofluorescence, D–I confocal microscopy). Scale bar, 10 μm. (For interpretation of the references to colour in this figure legend, the reader is referred to the web version of this article.)

there are age-, species-, or muscle type-specific differences in GNE expression. The significance of GNE double bands and differing apparent molecular weight of GNE in some organs remains to be determined. Posttranslational modifications could possibly account for differences in electrophoretic behavior as exemplified by in vitro phosphorylation of GNE [36]. Since GNE localizes in the cytosol, glycosylation is unlikely and was not confirmed by us (data not shown). Four different tissue-specific GNE mRNA-splice variants were suggested in human [37], corresponding to three GNE proteins with calculated molecular masses of the monomers of 79.2 kDa (variant I and IV), 82.5 kDa (variant II), and 74.6 kDa (variant III).

The GNE expression level is dependent on the differentiation state of the cell as evidenced by strong GNE Western blot signals in human embryonal cells and several cancer cell lines. These findings are consistent with elevated GNE mRNA levels found in early stages of mouse embryogenesis [33] and in various malignant human cell lines [34]. Also, most mouse tissues express low GNE protein levels. Upregulation of GNE in rapidly dividing and undifferentiated cells is consistent with the view that sialic acids are a universal marker of growing and developing

Fig. 7. Effects of brefeldin A (BFA) and nocodazole on the localization of GNE in human myoblasts and myotubes. Following BFA treatment (1 μg/ml) for 1 h, primary human myoblasts were double-immunolabeled with anti-GNE (A) and anti-golgin-97 (B) and analyzed by confocal immunofluorescence microscopy. Golgi-related structures are vesiculated or scattered throughout the cytoplasm. Superimposition of red (Texas Red) and green images (FITC) shows partial overlap of GNE and golgin-97 (C). Similarly, nocodazole treatment of primary myoblasts (30 μM) for 1.5 h results in the formation of multiple small vesicles derived from the Golgi compartment (E) most of which staining with the GNE antiserum (D–F). After recovery for 30 min following nocodazole treatment, the Golgi complex is not yet fully restored (G–I). Again, a partial overlap of GNE (G) and Golgi markers is observed (H, I). BFA treatment of differentiated, multinuclear myotubes (1 μg/ml) for 1 h disrupts juxtanuclear Golgi-related structures (K). GNE-specific staining appears diffusely distributed throughout the cytoplasm (J). The overlay reveals partial overlap of GNE and golgin-97 (L). Nocodazole treatment of myotubes (30 μM) for 1.5 h fails to disrupt the organization of the Golgi complexes. GNE (M) and golgin-97 (N) colocalize to juxtanuclear domains, often on opposite sides of the myonuclei (O). Scale bar, 10 μm. (For interpretation of the references to colour in this figure legend, the reader is referred to the web version of this article.)

tissues [38]. Moreover the extent of cell surface sialylation has been correlated to the metastatic potential of malignant cells [39].

GNE-specific immunolabeling of HeLa cells results in an intense staining of a polarized juxtanuclear compartment highly suggestive of the Golgi complex. Partial colocalization of GNE with markers of the Golgi apparatus including WGA, HPA, and golgin-97 is consistent with the view that GNE is a resident protein of the Golgi compartment or tightly associated to it. Our results suggest that GNE is not confined

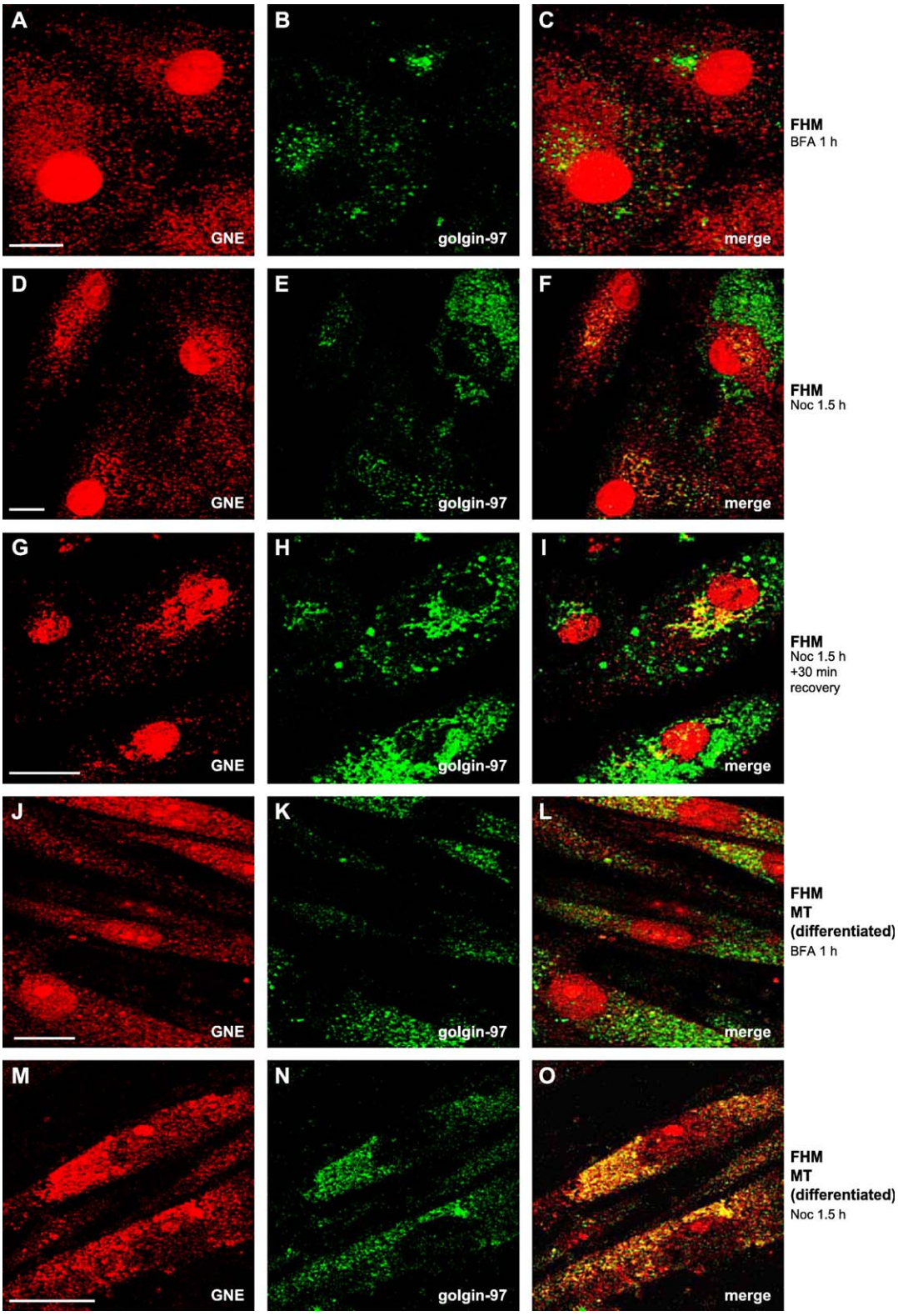

to *cis*-, *intermediate*-, or *trans*-Golgi but distributed throughout the entire Golgi compartment. Colocalization with specific marker proteins or electron microscopy studies will be required for more precisely localizing GNE to Golgi subcompartments. Also, it remains to be determined whether GNE resides in the Golgi lumen or on the cytosolic side of Golgi membranes. Since any significant GNE signal overlap with the endoplasmic reticulum was lacking as visualized by the marker enzyme PDI (protein disulfide isomerase), we exclude persistent targeting of GNE to the ER.

Since it is well established that mutations in GNE cause a rare inherited muscle disorder in humans called HIBM (OMIM 603824), muscle cells are of special interest regarding the subcellular distribution and regulation of GNE. We provide evidence that also human muscle cells, both differentiated and undifferentiated, reveal GNE localization to the Golgi. Consistent with previous detailed studies of Golgi complex reorganization during muscle differentiation [40], the Golgi compartment appears less compact, loses its polarized localization and distributes in a more perinuclear fashion in myotubes.

Golgi-disturbing pharmacological agents have proven useful tools for gaining insight into basic mechanisms of organelle formation and maintenance in the secretory pathway (for review, see Ref. [41]). As followed by the Golgi-resident marker protein golgin-97 and confocal microscopy, partial Golgi association of the GNE immunofluorescence signal is maintained throughout drug treatment and during the recovery process, a behavior indicative of Golgi-resident proteins. Complete recovery was indicated by relocation of GNE together with Golgi markers to a polarized intensely staining juxtanuclear structure likely to constitute the rebuilt Golgi complex. Importantly, the association of GNE with the Golgi compartment was further corroborated with $(FLAG)_3$-tagged GNE recombinantly expressed in HeLa cells.

The mechanism how GNE is targeted and retained in the Golgi compartment remains elusive. Golgi localization may involve disparate regions of a protein rather than a single discrete signal (for review, see Ref. [42]). For Golgi-resident glycosyl transferases two basic models have been proposed. (i) N-terminal signal sequence adjacent to the transmembrane domain mediates Golgi-targeting. (ii) A subset of Golgi-resident proteins are recruited to the organelle by a process known as kin recognition that involves protein–protein interaction in the stem region of the protein (for review, see Ref. [43]). Hence, GNE targeting might depend on protein–protein interaction with other Golgi-resident proteins according to the kin recognition model mediating precise localization within the Golgi stacks. Alternatively, GNE might be anchored to Golgi membranes by covalently attached fatty acid chains like myristoyl or farnesyl. Finally, we cannot exclude the possibility of different GNE splice forms [37] mediating specific targeting to the cytoplasm or the nucleus. Mutational analysis will be needed to clarify this issue.

Surprisingly, GNE was detected in the nucleus of HeLa and muscle cells by confocal microscopy. The nuclear localization of GNE was further corroborated by cell fractionation and immunoblot analysis revealing regulation of GNE protein expression in the nucleus as well as in the cytoplasm. The nuclear staining pattern varied largely in form and intensity among cells of the same type. These findings may suggest cell cycle dependent regulation of GNE targeting. This view is supported by the redistribution behavior of GNE upon high-dose nocodazole treatment (30 μM) and recovery. In about half of the cells GNE is nearly absent from the nucleus or present in lower levels than in the other half of the cell population. Although the half life of GNE in HeLa cells remains to be determined, the predominant Golgi localization most likely results from redistribution involving nucleocytoplasmic shuttling rather than protein de novo synthesis in the cytoplasm. In the transfection experiment, $(FLAG)_3$-tagged GNE was efficiently targeted to the Golgi complex as well as the nucleus. However, recombinant GNE was found in the nucleus at lower levels than wild type GNE in HeLa. There are several explanations why recombinant GNE is less abundant in the nucleus of transfected cells when compared to wild type GNE. (i) Overexpression of GNE under a constitutively active CMV promoter may alter the balance between the cytoplasmic and nuclear GNE pool. (ii) The N-terminal $(FLAG)_3$-tag might interfere with nucleocytoplasmic shuttling. (iii) Alternative splicing may give rise to variant GNE isoforms as previously suggested [37]. The transfected GNE construct represents only splice variant IV that might have a restricted subcellular distribution. Since the polyclonal GNE antibody was raised against an amino acid sequence in the C-terminal part of GNE within the kinase domain, all isoforms are recognized by the antibody.

Immunolocalization of wild type GNE consistently resulted in a prominent nuclear signal in the majority of cells. However, nuclear GNE staining was variable indicating differential regulation. We hypothesized that GNE might be a nucleocytoplasmic shuttling protein. A key feature of nucleocytoplasmic shuttling is the recognition of specific signals present in the substrate proteins. Although there are several candidate regions consisting of small basic amino acid clusters, no classical monopartite or bipartite nuclear localization signal (NLS) can be pinpointed in GNE [27]. However, protein export from the nucleus is often mediated by a leucine-rich nuclear export signal (NES). Visual inspection of the amino acid sequence identified a putative leucine-rich NES in agreement with the widely accepted consensus L-x(2,3)-[LIVFM]-x(2,3)-L-x-[LI] [44] suggesting that GNE might be a nucleocytoplasmic shuttling protein. Experimental evaluation is needed to support this hypothesis. The NES is highly conserved in GNE of human, mouse, rat, hamster and zebrafish (Fig. 8).

Several reasons are conceivable for nucleocytoplasmic shuttling of GNE. (i) Sialylation is considered the final step in the glycosylation of N- and O-linked oligosaccharides

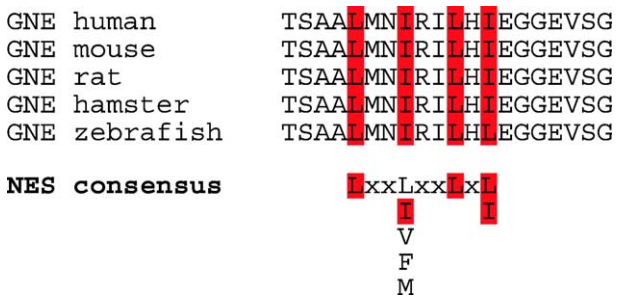

Fig. 8. Putative nuclear export signal in GNE. Sequence alignment of GNE homologues indicates a highly conserved putative leucine-rich nuclear export signal (NES) in amino acids 121–140 in accordance to the widely accepted consensus L-x(2,3)-[LIVFM]-x(2,3)-L-x-[LI]. The residues comprising the putative NES are shaded in red. (For interpretation of the references to colour in this figure legend, the reader is referred to the web version of this article.)

and is believed to occur either in the *trans*-cisternae or the *trans*-Golgi network [45]. Our data presented here suggest GNE localization in the Golgi compartment. Moreover, sialic acids are taken up as activated nucleotide donors, concentrated by specific transporters and consumed by specific glycosyltransferases during addition to glycoconjugate acceptors in the Golgi.

(ii) The substrate required for the addition of sialic acid to the terminal sugar residues of glycoproteins or gangliosides is provided by CMP-Neu5Ac synthetase that catalyzes the activation of Neu5Ac to CMP-Neu5Ac. For unknown reasons, this particular step takes place in the nucleus where also CMP-Neu5Ac synthetase was detected [18,19]. It is possible that GNE might travel to the nucleus to activate sialic acid biosynthesis within a large multi-enzyme complex containing the required machinery including CMP-Neu5Ac synthetase.

(iii) High levels of CMP-Neu5Ac, the final product of the sialic acid biosynthetic pathway allosterically regulate GNE by feedback inhibition [46,15]. Localization of GNE at the site of CMP-Neu5Ac consumption might relieve feedback inhibition thereby initiating sialic acid biosynthesis if the CMP-Neu5Ac concentration is low.

Compartmentalization of the cellular GNE pool might provide additional possibilities to regulate the enzyme's catalytic activities. Homology search of databases revealed significant homology of a series of bacterial xylose operon repressor proteins and ROK family transcriptional activators to the kinase domain of GNE [47]. It was speculated that the bicistronic vertebrate GNE gene evolved from two separate bacterial ancestor genes, an epimerase and a kinase activity. From an evolutionary point of view, GNE might play a role in modulating gene expression when targeted to the nucleus. The subnuclear staining pattern of GNE features widespread nucleoplasmic staining in addition to signal accumulation in a few large round shaped subnuclear domains. Colocalization experiments with established nuclear proteins might help to identify GNE interacting partners thereby pointing to yet unknown roles of the enzyme in the nuclear metabolism.

Immunofluorescence microscopy showing a static steady state snapshot of the cell, might fail to reveal transient subcellular localization of GNE. It remains to be determined whether allosteric end product inhibition of GNE regulates directional trafficking of the protein in addition to enzymatic activity. Our results suggest a dynamic localization with GNE moving in a temporal sequence between several subcellular compartments before adopting a steady state. The putative cycling behavior of GNE underlines the importance of measuring the dynamic properties of the protein in further detail when interpreting both GNE localization pattern and its possible functional implications. In vivo labeling of GNE by GFP fusion may allow to measure dynamic parameters directly and to dissect functional domains essential for precise subcellular targeting. Finally, elucidating how GNE targeting and function are dynamically linked may help to develop a model of how sialic acid biosynthesis is regulated and promote our understanding of the pathogenesis of human GNE-related disorders.

Acknowledgments

We are grateful to Eva Schmidtmayer and Eva Wiens for expert technical assistance. Human myoblast cultures were obtained from the Muscle Tissue Culture Collection at the Friedrich-Baur-Institute (Department of Neurology, Ludwig-Maximilians-University, Munich, Germany). The Muscle Tissue Culture Collection is part of the German network on muscular dystrophies (*MD-NET*, service structure S1, 01GM0302) funded by the German ministry of education and research (BMBF, Bonn, Germany). The Muscle Tissue Culture Collection is a partner of Eurobiobank (Eurordis; scientific coordinator: C. Jaeger, Paris, France) funded by the EC within the 5th framework (QLRT-2001-02769). SK receives a scholarship from The Myositis Association (Harrisonburg, VA, U.S.A.). This work was supported in part by grants from the Deutsche Forschungsgemeinschaft, Bonn, Germany to H.L. and R.H., from the Fritz-Thyssen-Stiftung, Köln, Germany and the German-Israeli Foundation for Scientific Research and Development, Jerusalem, Israel to S.H., Z.A. and S. M.-R. and the Sonnenfeld-Stiftung, Berlin, Germany, to S.H. and R.H.

References

[1] S. Rens-Domiano, T. Reisine, Structural analysis and functional role of the carbohydrate component of somatostatin receptors, J. Biol. Chem. 266 (1991) 20094–20102.
[2] G.M. Edelman, K.L. Crossin, Cell adhesion molecules: implications for a molecular histology, Annu. Rev. Biochem. 60 (1991) 155–190.
[3] A. Varki, Sialic acids as ligands in recognition phenomena, FASEB J. 11 (1997) 248–255.
[4] S. Kelm, R. Schauer, Sialic acids in molecular and cellular interactions, Int. Rev. Cytol. 175 (1997) 137–240.

[5] P.R. Crocker, Siglecs: sialic acid binding immunoglobulin-like lectins in cell–cell interactions and signalling, Curr. Opin. Struct. Biol. 12 (2002) 609–615.
[6] D. Vestweber, J.E. Blanks, Mechanisms that regulate the function of the selectins and their ligands, Physiol. Rev. 9 (1999) 181–213.
[7] D. Vestweber, Lymphocyte trafficking through blood and lymphatic vessels: more than just selectins, chemokins and integrins, Eur. J. Immunol. 33 (2003) 1362–1365.
[8] D.A. Alexander, K. Dimock, Sialic acid functions in enterovirus 70 binding and infection, J. Virol. 76 (2002) 11265–11272.
[9] M. Matrosovich, H.D. Klenk, Natural and synthetic sialic acid-containing inhibitors of influenza virus receptor binding, Rev. Med. Virol. 13 (2003) 85–97.
[10] H.H. Tong, X. Liu, Y. Chen, M. James, T. Demaria, Effect of neuraminidase on receptor-mediated adherence of *Streptococcus pneumoniae* to chinchilla tracheal epithelium, Acta Oto-Laryngol. 122 (2002) 413–419.
[11] J.W. Dennis, S. Laferte, Recognition of asparagine-linked oligosaccharides on murine tumor cells by natural killer cells, Cancer Res. 45 (1985) 6034–6040.
[12] R. Sawada, S. Tsuboi, M. Fukuda, Differential E-selectin-dependent adhesion efficiency in sublines of a human colon cancer exhibiting distinct metastatic potentials, J. Biol. Chem. 269 (1994) 1425–1431.
[13] M. Schwarzkopf, K.P. Knobeloch, E. Rohde, S. Hinderlich, N. Wiechens, L. Lucka, I. Horak, W. Reutter, R. Horstkorte, Sialylation is essential for early development in mice, Proc. Natl. Acad. Sci. U. S. A. 99 (2002) 5267–5270.
[14] W. Reutter, R. Stäsche, P. Stehling, O. Baum, The biology of sialic acids: insight into their structure, metabolism and function in particular during viral infection, in: H.-J. Gabius, S. Gabius (Eds.), Glycosciences, Status and Perspectives, Chapman & Hall, Weinheim, Germany, pp. 245–259.
[15] S. Hinderlich, R. Stäsche, R. Zeitler, W. Reutter, A bifunctional enzyme catalyzes the first two steps in *N*-acetylneuraminic acid biosynthesis of rat liver, Purification and characterization of UDP-*N*-acetylglucosamine 2-epimerase/*N*-acetylmannosamine kinase, J. Biol. Chem. 272 (1997) 24313–24318.
[16] O.T. Keppler, S. Hinderlich, J. Langner, R. Schwartz-Albiez, W. Reutter, M. Pawlita, UDP-GlcNAc 2-epimerase: a regulator of cell surface sialylation, Science 284 (1999) 1372–1376.
[17] E.L. Kean, S. Roseman, The sialic acids: X. Purification and properties of cytidine 5′-monophosphosialic acid synthetase, J. Biol. Chem. 241 (1966) 5643–5650.
[18] A.K. Münster, M. Eckhardt, B. Potvin, M. Mühlenhoff, P. Stanley, R. Gerardy-Schahn, Mammalian cytidine 5′-monophosphate *N*-acetylneuraminic acid synthetase: a nuclear protein with evolutionarily conserved structural motifs, Proc. Natl. Acad. Sci. U. S. A. 95 (1998) 9140–9145.
[19] A.K. Münster, B. Weinhold, B. Gotza, M. Mühlenhoff, M. Frosch, R. Gerardy-Schahn, Nuclear localization signal of murine CMP-Neu5Ac synthetase includes residues required for both nuclear targeting and enzymatic activity, J. Biol. Chem. 277 (2002) 19688–19696.
[20] H. Fried, U. Kutay, Nucleocytoplasmic transport: taking an inventory, Cell. Mol. Life Sci. 60 (2003) 1659–1688.
[21] U. Fischer, J. Huber, W.C. Boelens, I.W. Mattaj, R. Lührmann, The HIV-1 Rev activation domain is a nuclear export signal that accesses an export pathway used by specific cellular RNAs, Cell 82 (1995) 745–783.
[22] W. Wen, J.L. Meinkoth, R.Y. Tsien, S.S. Taylor, Identification of a signal for rapid export of proteins from the nucleus, Cell 82 (1995) 463–473.
[23] A. Blume, D. Ghaderi, V. Liebig, S. Hinderlich, P. Donner, W. Reutter, L. Lucka, UDP-*N*-acetylglucosamine 2-epimerase/*N*-acetylmannosamine kinase, functionally expressed in and purified from *E. coli*, yeast and insect cells, Protein Expr. Purif. 35 (2004) 387–396.
[24] H. Lochmüller, T. Johns, E.A. Shoubridge, Expression of the E6 and E7 genes of human papillomavirus (HPV16) extends the life span of human myoblasts, Exp. Cell Res. 248 (1999) 186–193.
[25] P.K. Smith, R.I. Krohn, G.T. Hermanson, A.K. Mallia, F.H. Gartner, M.D. Provenzano, E.K. Fujimoto, N.M. Goeke, B.J. Olson, D.C. Klenk, Measurement of protein using bicinchoninic acid, Anal. Biochem. 150 (1985) 76–85.
[26] B.P. Zhou, Y. Liao, W. Xia, B. Spohn, M.H. Lee, M.C. Hung, Cytoplasmic localization of p21Cip1/WAF1 by Akt-induced phosphorylation in HER-2/neu-overexpressing cells, Nat. Cell Biol. 3 (2001) 245–252.
[27] M. Cokol, R. Nair, B. Rost, Finding nuclear localization signals, EMBO Rep. 1 (2000) 411–415.
[28] S. Hammarstrom, L.A. Murphy, I.J. Goldstein, M.E. Etzler, Carbohydrate binding specificity of four *N*-acetyl-D-galactosamine-"specific" lectins: *Helix pomatia* A hemagglutinin, soy bean agglutinin, lima bean lectin, and *Dolichos biflorus* lectin, Biochemistry 16 (1977) 2750–2755.
[29] H. Debray, D. Decout, G. Strecker, G. Spik, J. Montreuil, Specificity of twelve lectins towards oligosaccharides and glycopeptides related to *N*-glycosylproteins, Eur. J. Biochem. 117 (1981) 41–55.
[30] K.J. Griffith, E.K. Chan, C.C. Lung, J.C. Hamel, X. Guo, K. Miyachi, M.J. Fritzler, Molecular cloning of a novel 97-kD Golgi complex autoantigen associated with Sjögren's syndrome, Arthritis Rheum. 40 (1997) 1693–1702.
[31] F.A. Barr, A novel Rab6-interacting domain defines a family of Golgi-targeted coiled-coil proteins, Curr. Biol. 9 (1999) 381–384.
[32] D.M. Ferrari, H.D. Söling, The protein disulphide-isomerase family: unravelling a string of folds, Biochem. J. 339 (1999) 1–10.
[33] R. Horstkorte, S. Nöhring, N. Wiechens, M. Schwarzkopf, K. Danker, W. Reutter, L. Lucka, Tissue expression and amino acid sequence of murine UDP-*N*-acetylglucosamine-2-epimerase/*N*-acetylmannosamine kinase, Eur. J. Biochem. 260 (1999) 923–927.
[34] L. Lucka, M. Krause, K. Danker, W. Reutter, R. Horstkorte, Primary structure and expression analysis of human UDP-*N*-acetylglucosamine-2-epimerase/*N*-acetylmannosamine kinase, the bifunctional enzyme in neuraminic acid biosynthesis, FEBS Lett. 454 (1999) 341–344.
[35] R. Stäsche, S. Hinderlich, C. Weise, K. Effertz, L. Lucka, P. Moormann, W. Reutter, A bifunctional enzyme catalyzes the first two steps in *N*-acetylneuraminic acid biosynthesis of rat liver. Molecular cloning and functional expression of UDP-*N*-acetylglucosamine 2-epimerase/*N*-acetylmannosamine kinase, J. Biol. Chem. 272 (1997) 24319–24324.
[36] R. Horstkorte, S. Nöhring, K. Danker, K. Effertz, W. Reutter, L. Lucka, Protein kinase C phosphorylates and regulates murine UDP-*N*-acetylglucosamine-2-epimerase/*N*-acetylmannosamine kinase, FEBS Lett. 470 (2000) 315–318.
[37] G.D.J. Watts, M. Thorne, M.J. Kovach, A. Pestronk, V.A. Kimonis, Clinical and genetic heterogeneity in chromosome 9p associated hereditary inclusion body myopathy: exclusion of GNE and three other candidate genes, Neuromuscular Disord. 13 (2003) 559–567.
[38] G. Kohla, E. Stockfleth, R. Schauer, Gangliosides with O-acetylated sialic acids in tumors of neuroectodermal origin, Neurochem. Res. 27 (2002) 583–592.
[39] E. Gorelik, U. Galili, A. Raz, On the role of cell surface carbohydrates and their binding proteins (lectins) in tumor metastasis, Cancer Metastasis Rev. 20 (2001) 245–277.
[40] Z. Lu, D. Joseph, E. Bugnard, K.J. Zaal, E. Ralston, Golgi complex reorganization during muscle differentiation: visualization in living cells and mechanism, Mol. Biol. Cell 12 (2001) 795–808.
[41] A. Dinter, E.G. Berger, Golgi-disturbing agents, Histochem. Cell Biol. 109 (1998) 571–590.
[42] A.S. Opat, C. van Vliet, P.A. Gleeson, Trafficking and localisation of resident Golgi glycosylation enzymes, Biochimie 83 (2001) 763–773.

[43] K.J. Colley, Golgi localization of glycosyl transferases: more questions than answers, Glycobiology 7 (1997) 1–13.
[44] T. la Cour, R. Gupta, K. Rapacki, K. Skriver, F.M. Poulsen, S. Brunak, NESbase version 1.0: a database of nuclear export signals, Nucleic Acids Res. 31 (2003) 393–396.
[45] S. Pfeffer, Membrane domains in the secretory and endocytic pathways, Cell 21 (2003) 507–517.
[46] K. Kikuchi, S. Tsuiki, Purification and properties of UDP-N-acetylglucosamine 2′-epimerase from rat liver, Biochim. Biophys. Acta 327 (1973) 193–206.
[47] K. Effertz, S. Hinderlich, W. Reutter, Selective loss of either the epimerase or kinase activity of UDP-*N*-acetylglucosamine 2-epimerase/*N*-acetylmannosamine kinase due to site-directed mutagenesis based on sequence alignments, J. Biol. Chem. 274 (1999) 28771–28778.